J|A|C|S COMMUNICATIONS

Published on Web 12/17/2008

Naphthalenedicarboximide- vs Perylenedicarboximide-Based Copolymers. Synthesis and Semiconducting Properties in Bottom-Gate N-Channel Organic Transistors

Zhihua Chen, Yan Zheng, He Yan, and Antonio Facchetti*

Polyera Corporation, 8045 Lamon Avenue, Skokie, Illinois 60077

Received July 12, 2008; E-mail: afacchetti@polyera.com

Organic thin-film transistors (OTFTs) based on molecular and polymeric semiconductors have attracted great scientific interest in the quest for "plastic" electronics.[1] The typical OTFT structure includes the source, drain, and gate contacts, a semiconductor layer, and a dielectric layer separating the gate from the semiconductor (Figure 1 for a bottom-gate device). Depending on the semiconductor majority charge transport efficiencies, the OTFT functions as a p-channel (hole-transporter)[2] or n-channel (electron-transporter)[3] switch. The key device performance parameters include the field-effect mobility (μ) and the current on−off ratio (I_{on}:I_{off}). To enable OTFT-based applications, these parameters should surpass those of amorphous silicon for devices fabricated/functioning in ambient.[1] Several p- and n-channel molecular semiconductors have achieved acceptable device performance and stability. For example, OTFTs based on acenes and oligothiophenes (p-channel) and perylenes (n-channel) exhibit $\mu > 0.5$ cm^2/V•s in ambient.[1−3] In recent years, high-performance p-channel polymers with $\mu > 0.1$ cm^2/V•s have been discovered, with those based on the thiophene core being by far the most investigated.[4] Despite impressive progress,[5] n-channel polymers for OTFTs remain problematic due to poor processability and/or negligible electron mobilities in ambient conditions.

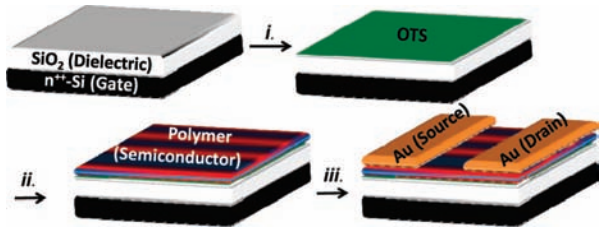

Figure 1. Schematic representation of the OTFT components and bottom-gate device structure investigated in this study. (*i*) Dielectric surface treatment; (*ii*) polymer spin-coating; (*iii*) Au contact deposition.

Among the most interesting electron-depleted cores used for n-channel polymer building blocks, perylenes have demonstrated the greatest potential.[5a,b] TFTs based on these polymers exhibit very promising electron mobilities in vacuum (0.001−0.02 cm^2/V•s); unfortunately, the corresponding devices do not operate in ambient.[5a,b] These fundamental results prompted us to design and explore new electron-depleted rylene-based polymers to enable high-performance n-channel polymeric TFTs. Here we report the synthesis and characterization of a *N*,*N*′-dialkylperylenedicarboximide-dithiophene (PDIR-T2) and *N*,*N*′-dialkylnaphthalenedicarboximide-dithiophene (NDIR-T2) copolymers and the fabrication of the corresponding bottom-gate TFTs on Si-SiO_2 substrates. To establish structure−property correlations within the rylene-based polymer family, the corresponding formal rylene NDIR and PDIR co-monomers were synthesized as well. Our results demonstrate that the choice of the NDIR vs PDIR co-monomer is strategic to achieve both high-performance n-channel TFTs and stable device operation in ambient conditions.

Following are the rylene building block and the polymer structural design rationale: (i) The electron-poor NDIR co-monomer was selected because of the large electron affinity of this core, comparable to that

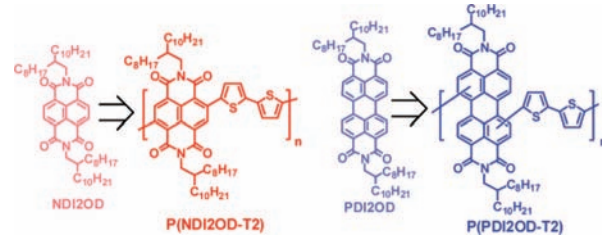

of the far more π-extended PDIR systems.[3d] (ii) Equally important, NDIR-Br_2 can be easily isolated as pure 2,6-diastereoisomers,[6a] enabling the synthesis of a regioregular polymeric backbone. Note that isolation of PDIR-Br_2 regioisomers is tedious.[6b] Therefore, compared to PDIR-based polymers, it should lead to a more π-conjugated structure and, consequently, better charge transport efficiencies. (iii) Proper alkyl (R) functionalization at the rylene nitrogen atoms, here 2-octyldodecyl (2OD), should result in highly soluble and processable, yet charge transport-efficient, polymers. (iv) The dithiophene (T2) unit is utilized because of the commercial availability, stability, and known electronic structure and geometric characteristics of this core,[7] likely providing highly conjugated, planar, and rod-like polymers.

Scheme 1. Synthesis of **P(NDI2OD-T2)** and **P(PDI2OD-T2)**

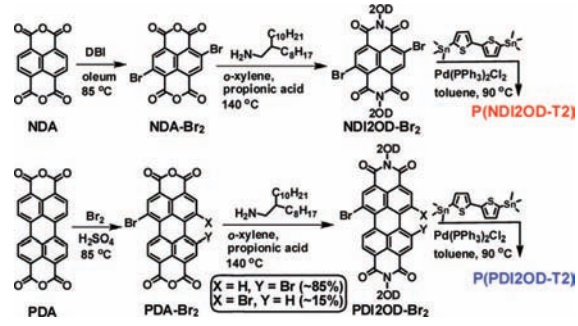

The new NDIR- and PDIR-based polymers [poly{[*N*,*N*′-bis(2-octyldodecyl)-1,4,5,8-naphthalenedicarboximide-2,6-diyl]-*alt*-5,5′-(2,2′-bithiophene)}, **P(NDI2OD-T2)** (Polyera ActivInk N2200), and poly{[*N*,*N*′-bis(2-octyldodecyl)-3,4,9,10-perylenedicarboximide-(1,7&1,6)-diyl]-*alt*-5,5′-(2,2′-bithiophene)} **P(PDI2OD-T2)**] were synthesized in high yields via a Pd-catalyzed Stille polymerization (according to Scheme 1 whereas synthetic details of **NDI2OD** and **PDI2OD** are reported in the Supporting Information). The new polymers were purified by multiple dissolution−precipitation procedures whereas **NDI2OD** and **PDI2OD** were by column chromatography and characterized by elemental analysis, gel permeation chromatography, and ^{1}H NMR spectroscopy. Using the reported synthetic procedure, polymer M_w's are larger for **P(NDI2OD-T2)** (~250K, PD ~ 5) than for **P(PDI2OD-T2)** (~32K, PD ~ 3).

The optical and electrochemical properties of these new systems reveal important aspects of the polymer electronic structures and NDIR vs PDIR co-monomer effects. The thin-film polymer optical absorption spectra exhibits two/three main absorptions located at λ_{max} = 697/391 nm for

10.1021/ja805407g CCC: $40.75

P(NDI2OD-T2) and λ_{max} = 594/540/360 nm for **P(PDI2OD-T2)** (Figure 2A). The corresponding (optical) energy gaps (E_g) are estimated from the spectrum low-absorption band edge as ~1.45 and 1.65 eV, respectively. Note that the E_g contraction (ΔE_g) on going from the formal **NDI2OD** and **PDI2OD** rylene monomer units ($E_g \approx 3.0$ and 2.4 eV, respectively) to the corresponding polymers is far larger for **P(NDI2OD-T2)** ($\Delta E_g \approx 1.65$ eV) than **P(PDI2OD-T2)** ($\Delta E_g \approx 0.75$ eV). The low E_g and the large ΔE_g for **P(NDI2OD-T2)** corroborate the extended/regioregular π-conjugated backbone and the efficient donor (T2)−acceptor (NDI) nature of this polymer when compared to regioirregular **P(NDI2OD-T2)**. Polymer thin-film cyclic voltammetry plots exhibit two reversible reductions (Figure 2B), with the first/second reduction potentials located at −0.49/−0.96 V for **P(NDI2OD-T2)** and at −0.44/−0.80V for **P(PDI2OD-T2)**. By combining solid-state optical and electrochemical data, the HOMO/LUMO energies (E_H/E_L) are found to be −5.36/−3.91 eV for **P(NDI2OD-T2)** and −5.61/−3.96 eV for **P(PDI2OD-T2)**. From previously established LUMO energy-stability correlations, E_L values are borderline for TFT ambient operation.[3d] Interestingly, when comparing rylene monomer vs polymer MO energies (Figure 2C), E_L's are structure-independent, whereas E_H's vary considerably. MO computations may shed light on these interesting trends; however, it is likely that they reflect the interplay between MOs' localization (LUMO primarily on the dicarboximide acceptor units and HOMO within the T2-arene polymeric backbone), NDI vs PDI core extension, and degree of polymer chain π-conjugation, as seen in donor−acceptor copolymers.[8]

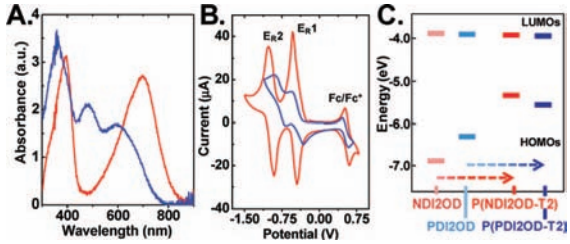

Figure 2. (A) Optical absorption spectra of spin-coated **P(NDI2OD-T2)** (red line) and **P(PDI2OD-T2)** (blue line) films (~30 nm thick) on glass. (B) Thin-film cyclic voltammetries [Fc (+0.54 V vs SCE) internal standard)] of **P(NDI2OD-T2)** (red line) and **P(PDI2OD-T2)** (blue line) thin films on a Pt electrode. The E_R1 values of **NDI2OD** and **PDI2OD** (not shown) are −0.49 and 0.46 V vs SCE, respectively. (C) Energy diagram for the specified rylene monomers and polymers.

Bottom-gate top-contact OTFTs were fabricated on n^{2+}-Si/SiO_2/OTS substrates on which the semiconducting polymer solutions (~3−10 mg/mL in DCB−$CHCl_3$) were spin-coated to afford ~100-nm-thick films. The films were annealed at 110 °C for 4 h before the TFT structure was completed by Au source/drain vapor deposition (Figure 1). Electrical measurements were performed both under high vacuum and in ambient. $I-V$ plots are shown in Figure 3, with μ calculated in saturation from the equation $\mu = (2I_{SD}L)/[WC_i(V_{SG} - V_{th})^2]$. The positive gate and source−drain voltages show that these polymers are n-channel semiconductors. Electron mobilities of ~0.06 $cm^2/V\cdot s$ for **P(NDI2OD-T2)** and ~0.002 $cm^2/V\cdot s$ for **P(PDI2OD-T2)** are measured in a vacuum. However, when the same TFT array is measured in ambient, the **P(NDI2OD-T2)**-based devices function 14 weeks after fabrication ($\mu \approx 0.01$ $cm^2/V\cdot s$), while the mobility of **P(PDI2OD-T2)** drops to ~2×10^{-4} $cm^2/V\cdot s$ within 1 week, in agreement with previous studies.[5] To our knowledge, **P(NDI2OD-T2)** is one of the very few n-channel polymers with good performance in ambient. Because of the good **P(NDI2OD-T2)**-based TFT electron injection characteristics from high workfunction contacts (Au), this material may open the door for all-polymer-based complementary circuits.

In summary, we have reported new rylene-based compounds for TFTs and demonstrated that the selection of the rylene electron-poor unit is essential to achieve high M_w, excellent π-conjugation, and good TFT performance in ambient conditions. Studies are underway of the effect of polymer regioregularity vs TFT performance and to enhance μ by *N*-substituent variations, co-monomer selection, and use of different dielectric materials and TFT structure.[9]

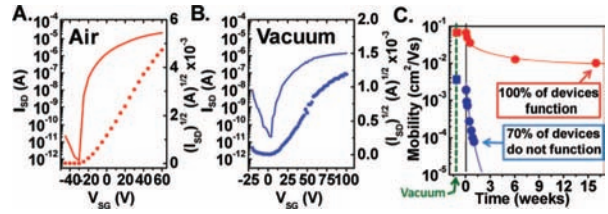

Figure 3. $I-V$ transfer plots for (A) **P(NDI2OD-T2)** TFT in air for 1 h and (B) **P(PDI2OD-T2)** TFT in vacuum. (C) Polymer TFT electron mobility plots in vacuum and ambient (RH = 20−40%, $T \approx 25$ °C) vs time.

Acknowledgment. We thank Prof. T. J. Marks and the BASF Printed Electronics team for helpful discussions.

Supporting Information Available: Polymer/monomer synthesis and characterization and device fabrication details. This material is available free of charge via the Internet at http://pubs.acs.org.

References

(1) (a) Allard, S.; Forster, M.; Souharce, B.; Thiem, H.; Scherf, U. *Angew. Chem., Int. Ed.* **2008**, *47*, 4070. (b) Mas-Torrent, M.; Rovira, C. *Chem. Soc. Rev.* **2008**, *37*, 827. (c) Cornil, J.; Bredas, J.-L.; Zaumseil, J.; Sirringhaus, H. *Adv. Mater.* **2007**, *19*, 1791. (d) Murphy, A. R.; Frechet, J. M. J. *Chem. Rev.* **2007**, *107*, 1066. (e) Locklin, J.; Roberts, M.; Mannsfeld, S.; Bao, Z. *Polym. Rev.* **2006**, *46*, 79.

(2) (a) Casado, J.; Zgierski, M. Z.; Ruiz, D.; Mari, C.; Lopez Navarrete, J. T.; Mas-Torrent, M.; Rovira, C. *J. Phys. Chem. C* **2007**, *111*, 10110. (b) Zhang, M.; Tsao, H. N.; Pisula, W.; Yang, C.; Mishra, A. K.; Muellen, K. *J. Am. Chem. Soc.* **2007**, *129*, 3472. (c) Vaidyanathan, S.; Doetz, F.; Katz, H. E.; Lawrentz, U.; Granstrom, J.; Reichmanis, E. *Chem. Mater.* **2007**, *19*, 4676. (d) Anthony, J. E. *Chem. Rev.* **2006**, *106*, 5028. (e) Kastler, M.; Laquai, F.; Mullen, K.; Wegner, G. *Appl. Phys. Lett.* **2006**, *89*, 252103/1.

(3) (a) See, K. C.; Landis, C.; Sarjeant, A.; Katz, H. E. *Chem. Mater.* **2008**, *20*, 3609. (b) Yang, C.; Kim, J. Y.; Cho, S.; Lee, J. K.; Heeger, A. J.; Wudl, F. *J. Am. Chem. Soc.* **2008**, *130*, 6444. (c) Di, C.-A.; Li, J.; Yu, G.; Xiao, Y.; Guo, Y.; Liu, Y.; Qian, X.; Zhu, D. *Org. Lett.* **2008**, *10*, 3025. (d) Jones, B. A.; Facchetti, A.; Wasielewski, M. R.; Marks, T. J. *J. Am. Chem. Soc.* **2007**, *129*, 15259. (e) Kuo, M. Y.; Chen, H. Y.; Cao, I. *Chem.-Eur. J.* **2007**, *13*, 4750. (f) Chen, H. Z.; Ling, M. M.; Mo, X.; Shi, M. M.; Wang, M.; Bao, Z. *Chem. Mater.* **2007**, *19*, 816. (g) Tang, Q.; Li, H.; Liu, Y.; Hu, W. *J. Am. Chem. Soc.* **2006**, *128*, 14634. (h) Haddock, J. N.; Zhang, X.; Domercq, B.; Kippelen, B. *Org. Electron.* **2005**, *6*, 182. (i) Newman, C. R.; Frisbie, C. D.; da Silva Filho, D. A.; Bredas, J.-L.; Ewbank, P. C.; Mann, K. R. *Chem. Mater.* **2004**, *16*, 4436.

(4) (a) Ong, B. S.; Wu, Y.; Li, Y.; Liu, P.; Pan, H. *Chem. Eur. J.* **2008**, *14*, 4766. (b) Chabinyc, M. L.; Toney, M. F.; Kline, R. J.; McCulloch, I.; Heeney, M. *J. Am. Chem. Soc.* **2007**, *129*, 3226. (c) McCulloch, I.; Heeney, M.; Bailey, C.; Genevicius, K.; Macdonald, I.; Shkunov, M.; Sparrowe, D.; Tierney, S.; Wagner, R.; Zhang, W. M.; Chabinyc, M. L.; Kline, R. J.; Mcgehee, M. D.; Toney, M. F. *Nat. Mater.* **2006**, *5*, 328. (d) Boudreault, P.-L. T.; Wakim, S.; Blouin, N.; Simard, M.; Tessier, C.; Tao, Y.; Leclerc, M. *J. Am. Chem. Soc.* **2007**, *129*, 9125. (e) Heeney, M.; Bailey, C.; Genevicius, K.; Shkunov, M.; Sparrowe, D.; Tierney, S.; McCulloch, I. *J. Am. Chem. Soc.* **2005**, *127*, 1078.

(5) (a) Huttner, S.; Sommer, M.; Thelakkat, M. *Appl. Phys. Lett.* **2008**, *92*, 093302/1. (b) Zhan, X.; Tan, Z.; Domercq, B.; An, Z.; Zhang, X.; Barlow, S.; Li, Y.; Zhu, D.; Kippelen, B.; Marder, S. R. *J. Am. Chem. Soc.* **2007**, *129*, 7246. (c) Babel, A.; Jenekhe, S. A. *J. Am. Chem. Soc.* **2003**, *125*, 13656.

(6) (a) Jones, B. A.; Facchetti, A.; Marks, T. J.; Wasielewski, M. R. *Chem. Mater.* **2007**, *19*, 2703. (b) Wurthner, F.; Stepanenko, V.; Chen, Z.; Saha-Moller, C. R.; Kocher, N.; Stalke, D. *J. Org. Chem.* **2004**, *69*, 7933.

(7) Barbarella, G.; Melucci, M.; Sotgiu, G. *Adv. Mater.* **2005**, *17*, 1581.

(8) (a) *Handbook of Conducting Polymers*, erd ed.; Skotheim, T. A., Reynolds, J. R. Eds.; CRC Press: Boca Raton, 2007. (b) Zotti, G.; Zecchin, S.; Schiavon, G.; Berlin, A.; Pagani, G.; Borgonovo, M.; Lazzaroni, R. *Chem. Mater.* **1997**, *9*, 2876. (c) van Mullekom, H. A. M.; Vekemans, J. A. J. M.; Havinga, E. E.; Meijer, E. W. *Mater. Sci. Eng. R: Reports* **2001**, *R32*, 1. (d) Toussaint, J. M.; Bredas, J. L. *Synth. Met.* **1993**, *61*, 103.

(9) We have also measured very large and stable μ values (>0.1 $cm^2/V\cdot s$) in ambient for **P(NDI2OD-T2)**-based top-gate TFTs. Yan, H.; Chen, Z.; Zheng, Y.; Newman, C.; Quinn, J. R.; Doltz, F.; Kestler, M.; Facchetti, A. *Nature*, in press.

JA805407G